AMERICAN SOCIETY FOR MICROBIOLOGY | mBio®

RESEARCH ARTICLE
Molecular Biology and Physiology

Genetic and Biochemical Analysis of Anaerobic Respiration in *Bacteroides fragilis* and Its Importance *In Vivo*

Takeshi Ito,[a] Rene Gallegos,[b] Leigh M. Matano,[c] Nicole L. Butler,[a,d] Noam Hantman,[a,e] Matthew Kaili,[b] Michael J. Coyne,[c] Laurie E. Comstock,[c] Michael H. Malamy,[b] Blanca Barquera[a,e]

[a]Center for Biotechnology and Interdisciplinary Sciences, Rensselaer Polytechnic Institute, Troy, New York, USA
[b]Department of Molecular Biology and Microbiology, Tufts University School of Medicine, Boston, Massachusetts, USA
[c]Division of Infectious Diseases, Brigham and Women's Hospital, Harvard Medical School, Boston, Massachusetts, USA
[d]Department of Chemistry and Chemical Biology, Rensselaer Polytechnic Institute, Troy, New York, USA
[e]Department of Biological Sciences, Rensselaer Polytechnic Institute, Troy, New York, USA

ABSTRACT In bacteria, the respiratory pathways that drive molecular transport and ATP synthesis include a variety of enzyme complexes that utilize different electron donors and acceptors. This property allows them to vary the efficiency of energy conservation and to generate different types of electrochemical gradients (H^+ or Na^+). We know little about the respiratory pathways in *Bacteroides* species, which are abundant in the human gut, and whether they have a simple or a branched pathway. Here, we combined genetics, enzyme activity measurements, and mammalian gut colonization assays to better understand the first committed step in respiration, the transfer of electrons from NADH to quinone. We found that a model gut *Bacteroides* species, *Bacteroides fragilis*, has all three types of putative NADH dehydrogenases that typically transfer electrons from the highly reducing molecule NADH to quinone. Analyses of NADH oxidation and quinone reduction in wild-type and deletion mutants showed that two of these enzymes, Na^+-pumping NADH:quinone oxidoreductase (NQR) and NADH dehydrogenase II (NDH2), have NADH dehydrogenase activity, whereas H^+-pumping NADH:ubiquinone oxidoreductase (NUO) does not. Under anaerobic conditions, NQR contributes more than 65% of the NADH:quinone oxidoreductase activity. When grown in rich medium, none of the single deletion mutants had a significant growth defect; however, the double Δ*nqr* Δ*ndh2* mutant, which lacked almost all NADH:quinone oxidoreductase activity, had a significantly increased doubling time. Despite unaltered *in vitro* growth, the single *nqr* deletion mutant was unable to competitively colonize the gnotobiotic mouse gut, confirming the importance of NQR to respiration in *B. fragilis* and the overall importance of respiration to this abundant gut symbiont.

IMPORTANCE *Bacteroides* species are abundant in the human intestine and provide numerous beneficial properties to their hosts. The ability of *Bacteroides* species to convert host and dietary glycans and polysaccharides to energy is paramount to their success in the human gut. We know a great deal about the molecules that these bacteria extract from the human gut but much less about how they convert those molecules into energy. Here, we show that *B. fragilis* has a complex respiratory pathway with two different enzymes that transfer electrons from NADH to quinone and a third enzyme complex that may use an electron donor other than NADH. Although fermentation has generally been believed to be the main mechanism of energy generation in *Bacteroides*, we found that a mutant lacking one of the NADH:quinone oxidoreductases was unable to compete with the wild type in the mammalian gut, revealing the importance of respiration to these abundant gut symbionts.

Citation Ito T, Gallegos R, Matano LM, Butler NL, Hantman N, Kaili M, Coyne MJ, Comstock LE, Malamy MH, Barquera B. 2020. Genetic and biochemical analysis of anaerobic respiration in *Bacteroides fragilis* and its importance *in vivo*. mBio 11:e03238-19. https://doi.org/10.1128/mBio.03238-19.

Editor Derek R. Lovley, University of Massachusetts Amherst

Address correspondence to Blanca Barquera, barqub@rpi.edu.

This article is a direct contribution from Michael H. Malamy, a Fellow of the American Academy of Microbiology, who arranged for and secured reviews by Dan Fraenkel, Harvard Medical School, and Robert Gennis, University of Illinois at Urbana Champaign.

Received 10 December 2019
Accepted 13 December 2019
Published 4 February 2020

KEYWORDS *Bacteroides fragilis*, respiration, NQR, gut microbiota

Studies of basic metabolic and energy-generating processes in bacteria have made important contributions to our understanding of how bacteria live in communities (1–3), adapt to changing environments (4), cause disease (3–6), and interact with their hosts (7, 8). Over the last decade, the microbiotas of the human gut have been intensely studied, revealing the importance of these microbial communities to human health and development (9–16). Despite all that we have learned, we still know relatively little about the central metabolic processes of many of the predominant bacterial members of this ecosystem.

Bacteroides is an abundant Gram-negative genus of the human intestinal microbiota, with its members predicted to stably colonize the host over a lifetime (17). *Bacteroides* species are saccharolytic bacteria that utilize complex dietary polysaccharides and host glycans present in the colon as their main carbon and energy sources. The ability of *Bacteroides* to harvest, degrade, and import these polysaccharides has been an area of intense study, yielding a wealth of important data (reviewed in reference 18). However, we know much less about how energy is generated from these molecules.

Aerobic respiration and anaerobic respiration are major energy-generating pathways of bacteria and are also the primary pathways for recycling the essential redox substrate NADH. NADH is generated by oxidative pathways, such as glycolysis and the Krebs cycle, and must be recycled to NAD^+ to serve as the substrate for these pathways (19, 20). In the initial step of respiration, NADH dehydrogenases (NADH:quinone oxidoreductases) transfer electrons from NADH to quinone at the cell membrane, thus recycling NADH to NAD^+. In aerobic respiration, these electrons are then transferred from the reduced quinone to O_2 by means of various cytochrome oxidases (21). During anaerobic growth, electrons can be transferred to other terminal electron acceptors, such as fumarate, nitrate, or sulfate, by the action of membrane-bound reductase enzymes (22–25). These electron transfer steps produce significant amounts of energy, and NADH dehydrogenases and cytochrome oxidases are typically able to conserve this energy by pumping either H^+ or Na^+ from the cytoplasm to the periplasm, forming transmembrane electrochemical gradients (20, 21, 26–31). These gradients provide a driving force for cations to return from the periplasm to the cytoplasm and thus supply power for cellular processes, including the transport of substrates and the generation of ATP by membrane-bound ATP synthases (21, 32–35).

Three different NADH:quinone oxidoreductases have been described in bacteria, and each has different catalytic functions, cofactors, and evolutionary origins (reviewed in reference 20). H^+-pumping NADH:ubiquinone oxidoreductase (NUO), or complex I, is the best studied due to its presence in mitochondria, where it is the only NADH:quinone oxidoreductase and is thus essential for energy generation (20). NUO is widely present in bacteria, where it is a 10- to 14-subunit protein complex with a flavin mononucleotide (FMN) and several iron-sulfur centers as cofactors for redox reactions (36, 37). As NUO transfers electrons from NADH to quinone, it conserves energy by pumping H^+ from the cytoplasm to the periplasm (38). Another NADH dehydrogenase that is present in fewer bacterial species and that is somewhat sporadically distributed (39) is Na^+-pumping NADH:quinone oxidoreductase (NQR). This protein complex is comprised of six subunits with several flavins and an iron-sulfur cluster as redox cofactors (40). In many bacteria, NQR has been shown to conserve energy during electron transfer by pumping Na^+ across the membrane (41, 42). The third described NADH dehydrogenase involved in respiration, NADH dehydrogenase II (NDH2), is a single membrane-associated protein that binds flavin adenine dinucleotide (FAD) as a redox cofactor (43). NDH2 does not pump ions across the membrane during electron transport and therefore does not conserve energy, but it may function to recycle NADH to NAD^+ under conditions of high membrane potential (43).

Few studies have analyzed respiration in *Bacteroides* species (44–49). It has been shown that under anaerobic conditions, fumarate can serve as a terminal electron

acceptor, with fumarate reductase (FRD) transferring electrons from the reduced quinone, producing succinate (47, 48, 50). To our knowledge, no studies have analyzed NADH:quinone oxidoreductase activity in *Bacteroides* species, and the complexes involved in this important energy generation step in *Bacteroides* species are unknown. Phylogenetic studies have identified the genes for both NUO (51) and NQR (39) in the *Bacteroides* genome, but no detailed biochemical or mutational analyses have demonstrated the involvement of these complexes in respiration. NQR activity has been identified in the related organism *Prevotella copri*, where a study of central carbon metabolism found NADH:quinone oxidoreductase activity in isolated cell membranes (52). This activity was attributed to NQR, as several of the genes coding for NUO subunits are absent in *Prevotella copri*. Similar results have also been reported for *Prevotella bryantii* (53). In the oral bacterium *Porphyromonas gingivalis*, the RprY response regulator positively activates NQR by interacting with the promoter upstream of the *nqrA* gene (54), and under conditions of oxidative stress, the production of RprY decreases, as does the expression of *nqrA* (55). In addition, the RprY regulator of *P. gingivalis* was shown to bind the promoter region of the *nqr* operon of *Bacteroides fragilis*, suggesting that the regulation of this operon is similar in these two bacteria.

In addition to anaerobic respiration, *Bacteroides* species are also capable of aerobic respiration. When *Bacteroides* strains are grown under nanaerobic conditions (0.05 to 0.15% oxygen), similar to the conditions that may be present at the mucosal lining of the gut (56), oxygen can serve as the terminal electron acceptor. *Bacteroides* species contain cytochrome *bd* oxidase, a high-affinity oxidase that functions under low-oxygen conditions, transferring electrons from reduced quinone to oxygen, producing water (21, 57). During nanaerobic respiration in *Bacteroides*, cytochrome *bd* oxidase contributes to the proton motive force during electron transfer, thereby conserving energy (58).

Here, we show that *B. fragilis* has orthologs of all three diverse NADH:quinone oxidoreductases, NUO, NQR, and NDH2. Through the creation and analysis of single and double deletion mutants, combined with activity measurements of isolated membrane fractions, we show that both NQR and NDH2 have functional NADH dehydrogenase activity but that NUO does not. We found that a mutant lacking NQR was unable to compete with wild-type (WT) bacteria in a gnotobiotic mouse competitive colonization model. In contrast, a mutant lacking NUO showed no competitive colonization defect, while a mutant lacking NDH2 had a modest colonization defect. This is the first study demonstrating the importance of NQR to bacterial fitness in the colonization of a mammalian host. On the basis of these results, we propose a new paradigm of respiration in *Bacteroides* species that is more complex than previously appreciated, with NQR playing a critical role in energy generation.

RESULTS

Identification of putative NADH:quinone oxidoreductase genes in *B. fragilis*. Analysis of the genome sequence of *B. fragilis* strain 638R revealed that it contains each of three described types of NADH:quinone oxidoreductases: NUO (BF638R_0850-0841), NQR (BF638R_2136-2141), and NDH2 (BF638R_1612). Figure 1 shows the organization of each of these genes/operons compared to their organization in the corresponding regions of *Escherichia coli* for *nuo* and *ndh2* and of *Vibrio cholerae* for *nqr*, as *E. coli* lacks *nqr*. The three genes shown in green in the *E. coli nuo* operon but missing in the corresponding *B. fragilis* operon code for the soluble portion of the enzyme complex that includes the NADH binding site. The presence of genes for these three different types of electron transfer complexes suggests that *B. fragilis* has a respiratory chain more complicated than previously appreciated, containing enzymes that have been shown in other organisms to pump H^+ (NUO) or Na^+ (NQR), as well as NDH2, which was not previously reported in the *Bacteroidales*.

Measurement of NADH:quinone oxidoreductase activity of isolated membranes. To study the role of each of these enzymes in the respiration of *B. fragilis*, we made mutants with an internal deletion in each gene/operon, performed biochemical

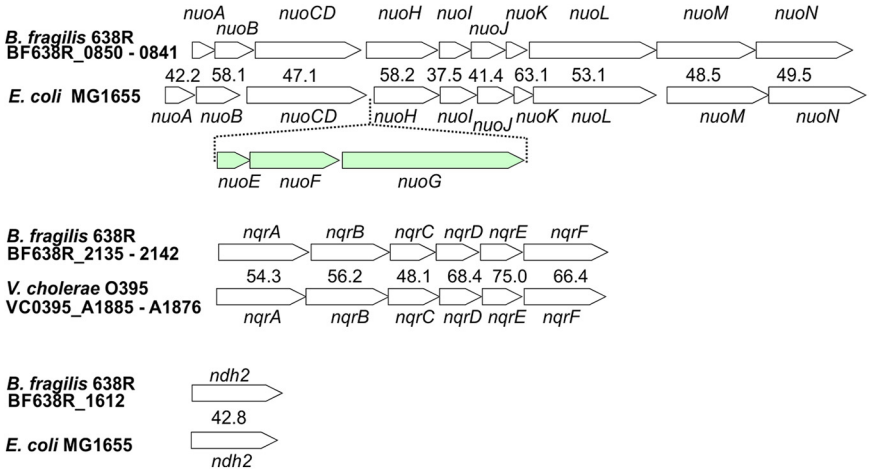

FIG 1 Identified operons of *B. fragilis* encoding predicted NADH:quinone oxidoreductases. The respective operons from *E. coli* or *V. cholerae* (*nqr*) are shown below each region, and the percent similarities of the products of the genes from these strains are listed. The *nuo* operon of *B. fragilis* is lacking three genes, shown in green, present in the *nuo* operon of *E. coli*.

activity measurements, and compared the NADH:quinone oxidoreductase activity in each of the mutants to that in the WT strain. Figure 2 shows measurements of NADH:quinone oxidoreductase activity measured in two ways: by the steady-state rates of NADH oxidation and by the reduction of menadione. For the *nuo* deletion mutant, there was no statistically significant difference in the activities in the mutant compared to that in the WT. This was the result that we predicted, based on the lack of *nuoEFG* in the *nuo* operon. In contrast, in the *ndh2* and *nqr* deletion mutants, the activities were significantly decreased and were approximately 78% and 42% of the WT values, respectively. These results strongly suggest that under the growth conditions used in these experiments, the NADH:quinone oxidoreductase activity of *B. fragilis* is a function of NQR and NDH2 in a roughly 2:1 ratio, with no contribution from NUO, as predicted based on the lack of *nuoEFG*. Full NADH:quinone oxidoreductase activity was restored in the *nqr* and *ndh2* complemented strains (Fig. 2A), indicating that the activity lost was due to these deletions.

Three double deletion mutants were created to provide more specific information about the contribution of each individual enzyme complex. As illustrated in Fig. 2B, each double deletion mutant could synthesize only one of the three enzymes, allowing measurements to focus on the activity of the one remaining enzyme (Fig. 2C). The activity in the Δ*ndh2* Δ*nuo* strain was approximately 61% of that in the WT, which was similar to that of the *ndh2* single deletion mutant, as expected, since we showed that the *nuo* single deletion mutant had full NADH:quinone oxidoreductase activity (Fig. 2A). Activity in the Δ*nuo* Δ*nqr* strain was approximately 36%, which was similar to that in the *nqr* single deletion mutant. These results strengthen our conclusion that NUO does not contribute to NADH:quinone oxidoreductase activity, as predicted. Furthermore, the Δ*nqr* Δ*ndh2* deletion mutant exhibited essentially no measurable activity (Fig. 2B), supporting the suggestion that NUO is not an NADH:quinone oxidoreductase in *B. fragilis*.

The Δ*nqr* Δ*ndh2* mutant was created by making an *ndh2* deletion in the Δ*nqr* strain. During resolution of the *ndh2* cointegrate, we noticed that both normal and small-size colonies were produced and determined that the small colonies were those of the Δ*nqr* Δ*ndh2* mutant (Fig. 2D). This growth defect likely results from the greatly reduced ability of this mutant to recycle NADH. In addition, this mutant likely obtains most of its energy by substrate-level phosphorylation, which yields less ATP per molecule of glucose, which may also contribute to the slower growth. When the *ndh2* operon was added back to the Δ*nqr* Δ*ndh2* mutant, the NADH:quinone oxidoreductase activity was recovered (Fig. 2B).

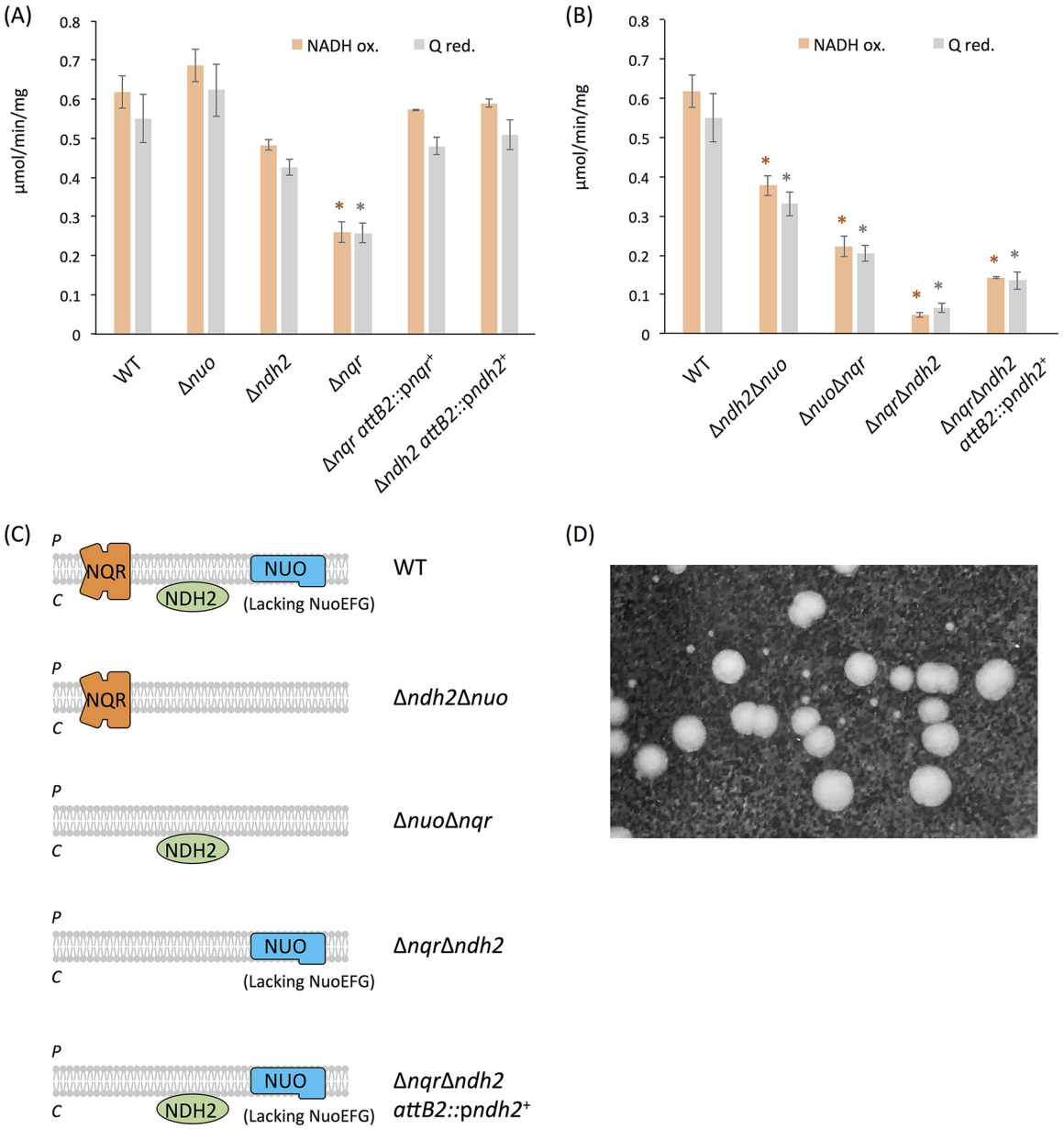

FIG 2 (A and B) NADH:quinone oxidoreductase activity in membranes of the *B. fragilis* WT (A and B), the single deletion mutant strains (the Δ*nuo*, Δ*ndh2*, and Δ*nqr* strains) and complemented strains (the Δ*nqr attB2*::p*nqr*$^+$ and Δ*ndh2 attB2*::p*ndh2*$^+$ strains) (A), and double deletion mutant strains (the Δ*ndh2* Δ*nuo*, Δ*nuo* Δ*nqr*, Δ*nqr* Δ*ndh2*, and Δ*nqr*Δ *ndh2 attB2*::p*ndh2*$^+$ strains) (B). The rates of NADH oxidation (NADH ox.; orange) and menadione (vitamin K_3) reduction (Q red.; gray) using NADH were measured. Mean values ($n = 3$ to 5 experiments) are presented, and error bars show the standard errors. Data were analyzed by Dunnett's test. *, $P < 0.05$ between the wild type and each mutant strain. (C) Diagram showing the enzyme that is present in each double mutant, i.e., the enzyme whose activity is measured. The letters P and C at the left-hand side of the membrane indicate the periplasm and cytoplasm, respectively. (D) Colony size comparison between the Δ*nqr* Δ*ndh2* mutant (small colonies) and the Δ*nqr* single-deletion-mutant parent strain (large colonies). The photograph was taken after 5 days of growth.

Use of NADH analogs. To further analyze the NADH:quinone oxidoreductase of *B. fragilis*, we utilized deamino-NADH (d-NADH), a substrate analog of NADH (Fig. 3). d-NADH has been widely reported in other species to donate electrons to NUO and NQR but not to NDH2 (59–61). This specificity makes it possible to discriminate between NDH2 activity and the other NADH dehydrogenase activities by comparing the activities with the two different substrates. To confirm that d-NADH has the same specificity in *B. fragilis*, we first measured the activities with each of the substrates in the two double deletion mutants that retained only one type of NADH:quinone oxidoreductase

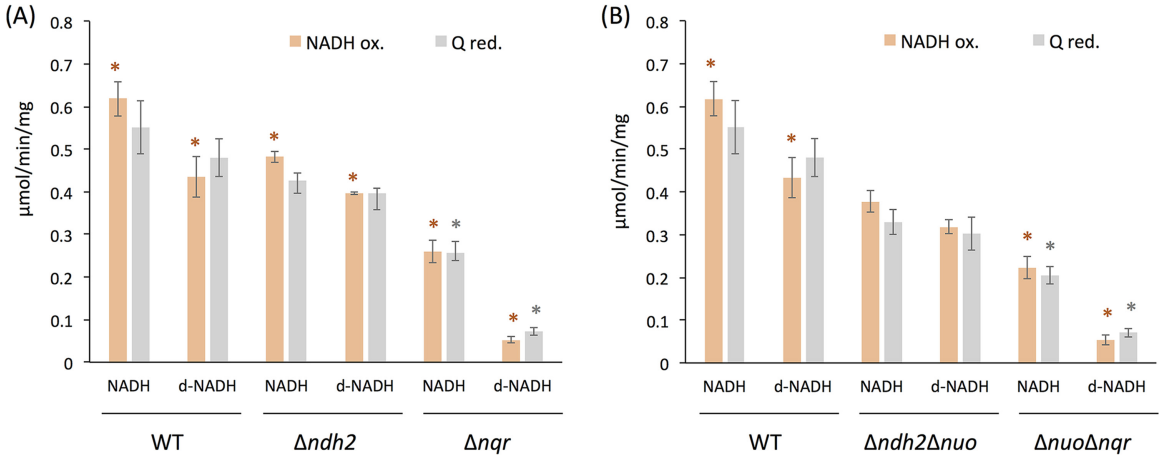

FIG 3 NADH:quinone oxidoreductase activities in membranes of the *B. fragilis* WT (A and B), the single deletion mutant strains (the Δ*ndh2* and Δ*nqr* strains) (A), and the double deletion mutant strains (the Δ*ndh2* Δ*nuo* and Δ*nuo* Δ*nqr* strains) (B), comparing NADH and deamino-NADH (d-NADH) as substrates. The rates of NADH oxidation (NADH ox.; orange) and menadione (vitamin K_3) reduction (Q red.; gray) using NADH or d-NADH were measured. Mean values and standard errors are from 3 to 5 experiments. Data were analyzed by an unpaired *t* test (*, $P < 0.05$) between NADH and d-NADH for each strain.

activity, the Δ*ndh2* Δ*nuo* mutant, which contains only *nqr*, and the Δ*nuo* Δ*nqr* mutant, which contains only *ndh2*, as well as the WT. In the WT and the mutant containing only *nqr*, the activities with d-NADH were slightly lower than those with NADH, consistent with reports that d-NADH is a slightly less efficient substrate. However, in the mutant containing only *ndh2*, the activity was almost completely absent. Thus, d-NADH can be used in *B. fragilis* to discriminate the NDH2 activity in the presence of other NADH: quinone oxidoreductases.

Based on this finding, we then used NADH and d-NADH to analyze single deletion mutants. The activity of the Δ*ndh2* mutant was approximately the same with either NADH or d-NADH, whereas the Δ*nqr* mutant was active with NADH but had very low activity with d-NADH. These results are another confirmation that *B. fragilis* NUO does not use NADH as an electron donor.

***In vitro* growth analysis of single and double deletion mutants.** We investigated the growth characteristics of the single and double deletions in rich medium under anaerobic conditions (Fig. 4; see also Table S1 in the supplemental material). With the exception of the Δ*nqr* Δ*ndh2* mutant, all of the strains had doubling times within 13% of the doubling time of the WT and reached similar maximum values of the optical density at 600 nm (OD_{600}) at the stationary-phase plateau. The Δ*nqr* Δ*ndh2* strain had a much longer doubling time (176 min) than the WT and an OD_{600} at the plateau of 70% of that of the WT. These changes were largely reversed when *ndh2* was reintroduced into the strain, yielding a much faster doubling time of 75 min (Fig. 4; Table S1).

Competitive colonization assays in gnotobiotic mice. As the *nqr*, *ndh2*, and *nuo* single deletion mutants did not demonstrate any significant *in vitro* growth defect compared to the growth of the WT, we tested their importance to bacterial fitness *in vivo*. For each mutant, competitive colonization assays (competing WT with the mutant) were performed using gnotobiotic mice (Fig. 5; Table S2). After a week of competitive colonization, we found that the Δ*nqr* mutant was outcompeted and was present as less than 1% of the total bacteria in the feces, as no Δ*nqr* mutants were detected in the more than 100 colonies analyzed for each mouse. The ability of this mutant to competitively colonize was reestablished to a large extent, although not completely, when the *nqr* operon was restored to the Δ*nqr* mutant. In contrast, the Δ*nuo* mutant showed no significant difference in colonization from that of the WT in the competitive colonization assay, while the Δ*ndh2* mutant showed a modest colonization defect, with the mutant colonization being reduced from 57.3% in the starting inoculum to 41.1% ± 4.1% (standard deviation) in the feces at 1 week ($P = 0.0002$). This colonization

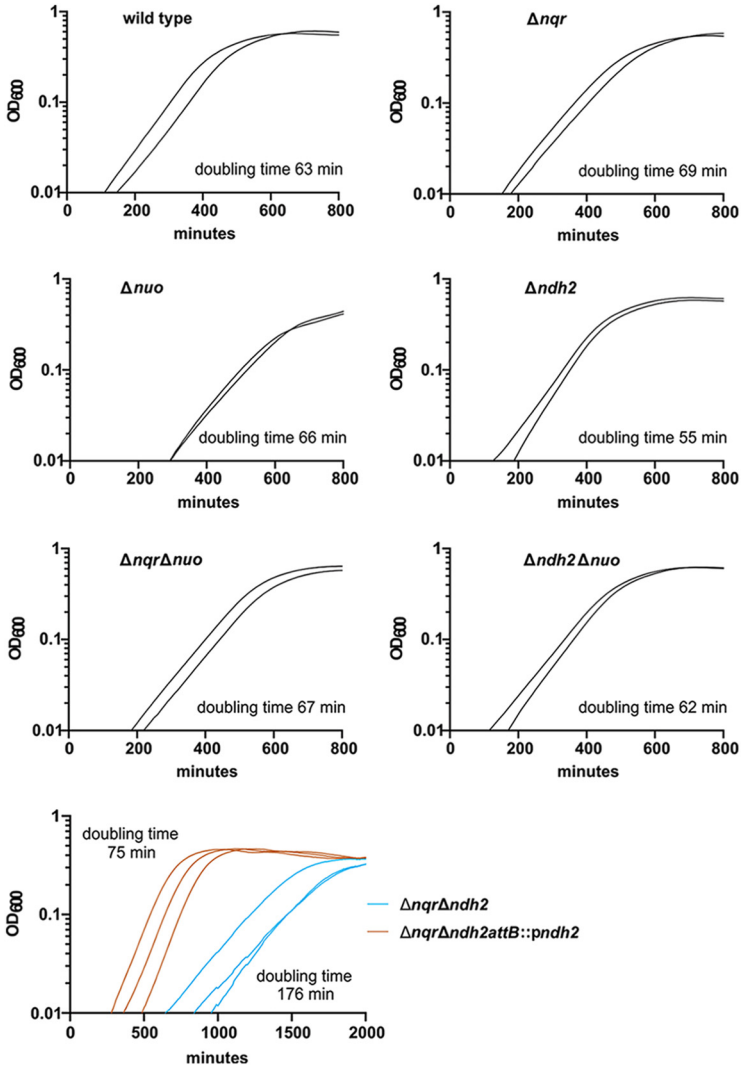

FIG 4 Growth curves for the WT, the single and double deletion mutants, and the Δ*nqr* Δ*ndh2 attB2*::p*ndh2*$^{+}$ strain in rich medium (BHIS medium) under anaerobic conditions. The growth of each strain (in duplicate or triplicate) was followed as the change in the absorbance at 600 nm in a BioTek plate reader. Doubling times were calculated as outlined in the Materials and Methods section, with all growth data being supplied in Table S1 in the supplemental material.

defect was also reversed when *ndh2* was added back to this mutant (Fig. 5). These data support the findings of the activity assays showing that NQR is the most active NADH:quinone oxidoreductase and the most important enzyme complex of the three studied for bacterial colonization in this model system.

DISCUSSION

In this study, we defined the enzymes involved in the crucial first step of respiration in *B. fragilis*, the transfer of electrons from NADH to quinone (Fig. 6). While all three typical classes of NADH dehydrogenases are present in *B. fragilis*, we found that only two have this activity. Under the growth conditions used in this study, NQR was the most active and the most important NADH:quinone oxidoreductase. Deletion of *nqr* resulted in a mutant that was severely attenuated for competitive colonization of the mouse intestine. A second enzyme, NDH2, could also catalyze this step and similarly had a competitive colonization defect, albeit not as severe as that of the Δ*nqr* mutant. In addition, *B. fragilis* has a homolog of complex I (NUO) for which we could not demonstrate NADH:quinone oxidoreductase activity, nor could we demonstrate a fitness defect of the Δ*nuo* mutant in the mouse colonization model.

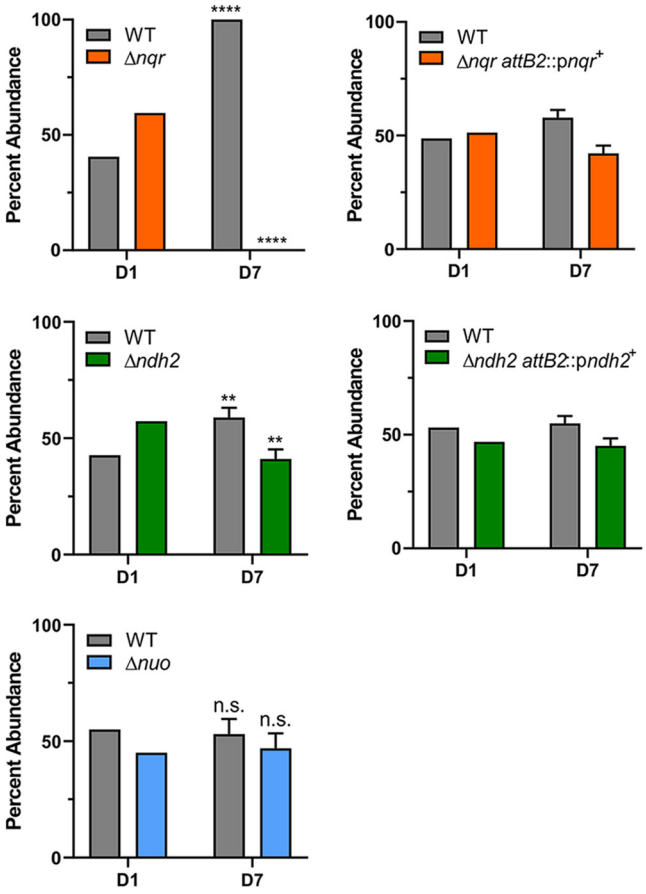

FIG 5 Mouse competitive colonization experiments with the *B. fragilis* WT and respiration mutants show fitness defects of the Δ*nqr* and Δ*ndh2* mutants. Data are representative results for the *B. fragilis* WT and respiration mutant Δ*nqr*, Δ*ndh2*, and Δ*nuo* strains or complemented Δ*nqr attB*::p*nqr*$^+$ and Δ*ndh2 attB*::p*ndh2*$^+$ strains in mouse gut colonization assays. The percentage of WT and mutant strains in the inoculum (day 1 [D1]) and feces (day [D7]) of the samples is shown as the mean and standard error of the mean (when applicable). The differences in abundance of the Δ*nqr* and the Δ*ndh2* mutants from days 1 to 7 were statistically significant (****, $P = 1E{-}40$; **, $P = 0.0002$), but they were not for the Δ*nuo* mutant ($P > 0.05$ [n.s., not significant]). All experiments were performed with 3 male and 3 female germfree Swiss Webster mice. The phenotype was replicated in both the males and the females, and the breakdown by sex is shown in Fig. S1 in the supplemental material.

The lack of NADH:quinone oxidoreductase activity of NUO may be attributable to poor expression of the *nuo* operon under the conditions of our assay. Our analysis of published transcriptome sequencing data (62) revealed that the *nuo* operon is in fact poorly expressed during anaerobic growth in rich medium. However, the lack of NADH

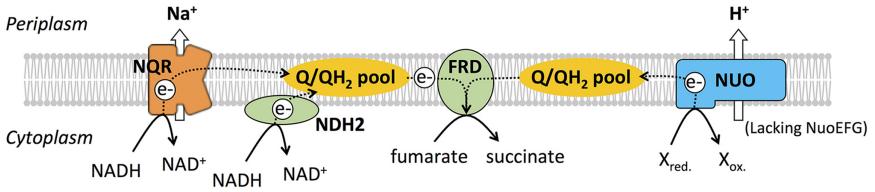

FIG 6 Current model of anaerobic respiration in *B. fragilis*. Substrate reactions and electron transfers are shown as solid and broken arrows, respectively. NQR and NDH2 oxidize NADH to NAD$^+$ and donate electrons to the menaquinone pool (Q/QH_2). Fumarate reductase (FRD) accepts electrons from reduced menaquinone and transfers them to the terminal electron acceptor, fumarate, which is reduced to succinate. *B. fragilis* NUO, lacking the NADH binding domain (NuoEFG subunits), likely oxidizes an unknown electron donor ($X_{red.}$) to transfer electrons via the menaquinone pool to FRD. In this scheme, energy is conserved when ion gradients are generated by NQR and NUO.

oxidation activity is likely also explained by NUO's unusual subunit composition. In comparison to the *nuo* operons of most bacteria, the *nuoE*, *nuoF*, and *nuoG* genes are missing in *B. fragilis* (Fig. 1). In a typical NUO complex, NuoE, NuoF, and NuoG make up a hydrophilic domain that includes the conserved NADH binding site. A NUO lacking this soluble domain should not be able to use NADH as a substrate. We analyzed 144 *B. fragilis* genomes and found that all have similar *nuo* operons lacking these three genes. The conservation of this operon in the species suggests that it has a different yet likely still important function in respiration. NUO complexes lacking these subunits have been described. The enzyme complex from *Prevotella copri* has the same 11-subunit organization as that from *B. fragilis* (52), while the enzyme from *Campylobacter jejuni* does not have NuoE and NuoF but retains NuoG, giving it a total of 12 subunits (52, 63). The more typical form of NUO, which uses NADH as a substrate, is exemplified by the complex from *E. coli*, with 14 subunits, including NuoE, NuoF, and NuoG (51). We predict that the *B. fragilis* NUO receives electrons from a distinct donor and transfers them to menaquinone while generating an H^+ motive force (Fig. 6).

NQR is found only in prokaryotes and is present in many marine and pathogenic bacteria. In most organisms where NQR has been studied, the enzyme operates as a primary Na^+ pump (64, 65). Our findings suggest that *Bacteroides* generates an Na^+ gradient directly through respiration by NQR, rather than depending completely on Na^+/H^+ antiporters to generate an Na^+ gradient. The primacy of NQR as the most active NADH:quinone oxidoreductase in *B. fragilis* and as the most important one for competitive colonization suggests that the Na^+ gradient likely has a key role in the production and distribution of energy in these bacteria. In fact, more than 10 genes annotated as encoding Na^+-dependent transporters are present in the *B. fragilis* 638R genome.

B. fragilis is also capable of aerobic respiration, employing the terminal oxidase cytochrome *bd*, which is expected to conserve energy in the form of an H^+ electrochemical membrane gradient (49, 57). We predict that nanaerobic respiration confers a fitness advantage in the oxygenated environment near the colonic mucus layer. Thus, to fully understand the respiratory pathways in *B. fragilis* and their importance in energy conservation under different environmental conditions in the gut, it will be important to also better define the properties and enzymes of this nanaerobic respiratory chain.

MATERIALS AND METHODS

Bacterial strains and growth conditions. For all studies, we used a strain of *B. fragilis* 638R (TM4000) and its *thy*-negative mutant (ADB77). The strains were grown anaerobically at 37°C in brain heart infusion supplemented (BHIS) medium containing 0.5% (wt/vol) yeast extract, 5 μg/ml hemin, and, when necessary, 50 μg/ml thymine, as well as antibiotics (5 μg/ml erythromycin, 200 μg/ml gentamicin, or 40 ng/ml anhydrotetracycline [aTC]). *Escherichia coli* strain S17 λ *pir* and derivatives were grown in LB broth or plates, with 100 μg/ml ampicillin or carbenicillin being added where appropriate. All strains and plasmids used are listed in Table S3 in the supplemental material.

Construction of deletion mutant strains. (i) *nqr* (BF638R_2136-2141) and *nuo* (BF638R_0841-0850) operon deletion. Upstream and downstream flanking regions of the *nqr* and *nuo* operons were amplified by PCR using the primers listed in Table S4 containing BamHI and NcoI sites for the upstream fragment and NcoI and HindIII sites for the downstream portion. These PCR products were digested and cloned by three-way ligation into BamHI-HindIII-digested pTY102 (66). The resulting plasmids were introduced into *B. fragilis* ADB77 by conjugation. Cointegrates were selected with erythromycin and gentamicin, and the cointegrate was passaged in nonselective medium and then plated on plates with 80 to 100 μg/ml trimethoprim and 50 μg/ml thymine to select against cointegrates (66). The resulting colonies were tested by PCR to differentiate mutant and WT resolvants. For animal experiments, the *thy* mutation in the background strain was restored to the WT by allelic exchange with the *thy*-positive suicide vector pYT102 (66).

(ii) Creation of pLGB36, an inducible counterselection vector for allelic deletions and replacements in *B. fragilis* 638R. Plasmid pLGB36 was made specifically to make allelic deletions and replacements in *B. fragilis* 638R and other *B. fragilis* strains that have the same type VI secretion system (T6SS) locus as strain 638R (67). This vector was created using the backbone of plasmid pLGB13 (68), which was designed for allelic replacements in *Bacteroides* and *Parabacteroides* species using the type VI secretion effector Bfe1 of strain 638R. As pLEC13 uses the 638R effector, strains with this T6SS region are immune to this toxin. In pLGB36, we used an effector from the T6SS region of *B. fragilis* strain S36_L11 (M136_1999), which we designated *bfe-3*, and replaced *bfe-1* and its engineered signal sequence of

pLGB13 with *bfe-3* with the same signal sequence to target the effector to the periplasm, where it is toxic upon induction with aTC. We have not found any resistance to this toxin, nor have we encountered the growth of any colonies that are not double-cross-out resolvants, demonstrating the utility of this vector for allelic deletions and replacements in strain 638R and others encoding the Bfe1 effector/immunity pair.

(iii) *ndh2* (BF638R_1612) deletion. The *ndh2* deletion was created using pLGB36. Upstream and downstream flanking regions were cloned into the BamHI site of pLGB36 using the NEBuilder assembly tool (New England Biolabs) with the primers listed in Table S4 and transformed into *E. coli* S17 λ *pir*. The construct was verified by whole-plasmid sequencing and transferred by conjugation into TM4000. Cointegrates were selected on BHIS medium plates with gentamicin and erythromycin. A cointegrate was grown in basal medium (69) for 5 h and then plated with 40 ng/μl aTC. Resolvants were screened by PCR and mutants were selected.

Complementation of mutant strains. (i) *nqr* operon complementation. The complete *nqr* operon with its native promoter (6,563 bp) was amplified by PCR using primers with a NotI restriction site at the 5′ end and a BamHI restriction site at the 3′ end (Table S4). The digested PCR product was cloned into NotI- and BamHI-digested pNBU2-*bla-ermGb*, which integrates into the chromosome and is tranformed into S17 λ *pir*. The construct was sequenced to confirm that no mutations were introduced. The plasmid was transferred by conjugation into the *nqr* deletion strain. Transconjugants with integration of the plasmid at the *attB2* site of tRNA-Ser were selected by PCR using the primers listed in Table S4.

(ii) *ndh2* complementation. The *ndh2* gene with its promoter was cloned into pNBU2-*bla-ermGb* using the NEBuilder assembly tool with the primers listed in Table S4 and transformed into S17 λ *pir*. The construct was verified by whole-plasmid sequencing. Transconjugants with integration of the plasmid at the *attB2* site of tRNA-Ser were selected by PCR, as described above.

Cell membrane preparation. All bacterial cultures were harvested in mid-logarithmic growth phase and washed with KPi buffer, containing 40 mM KH_2PO_4, pH 7, and 5 mM dithiothreitol. The cells were broken using a French press (24,000 lb/in^2, 2 cycles) under anaerobic conditions in KPi buffer containing DNase and phenylmethylsulfonyl fluoride (PMSF) protease inhibitor at 4°C. Broken cells were removed by centrifugation (3,800 × *g*), and the remaining supernatant was then centrifuged at 185,500 × *g* overnight to separate the inner membranes. The inner membrane preparations were washed and resuspended in KPi buffer under anaerobic conditions and stored at −80°C.

NADH:quinone oxidoreductase activity. The NADH:quinone oxidoreductase activity was followed spectrophotometrically at room temperature under an argon atmosphere in a buffer containing 50 mM Tris-HCl, pH 7, 1 mM EDTA, 100 mM NaCl, 5% (vol/vol) glycerol, 0.05% (wt/vol) *n*-dodecyl β-maltoside, 100 μM NADH, and 50 μM menadione (vitamin K_3). As it has been reported that menaquinone is the quinone produced by *B. fragilis* (70), menadione was used as the electron acceptor from NADH for all activity studies.

The oxidation of K_2-NADH or nicotinamide hypoxanthine dinucleotide, reduced-form Na^+ salt (deamino-NADH), was measured at 343 nm ($\varepsilon = 6.22\ mM^{-1}\ cm^{-1}$), where menadione and menadiol are isosbestic (71). The reduction of menadione was measured at 262 nm ($\varepsilon = 14.0\ mM^{-1}\ cm^{-1}$), and the results were adjusted by subtracting the calculated contribution of the accumulating NAD^+ from the total absorbance at 262 nm. The absorbance of NAD^+ at 262 nm ($\varepsilon = 17.8\ mM^{-1}\ cm^{-1}$) was calculated from the absorbance change at 343 nm. Membrane preparations from the WT or mutant strains were used at a protein concentration of 60 μg/ml. The reaction was initiated by adding membranes to the buffer containing 100 μM NADH and 50 μM vitamin K_3 under an argon atmosphere. All activity measurements were performed at least three times.

Growth analysis. Cultures of the wild-type and mutant strains described in this paper were grown in BHIS broth overnight, diluted 1 to 10 in fresh broth, and grown to mid-exponential phase. A suitable volume (usually 10 μl) was then used to inoculate 1 ml of prereduced BHIS broth in wells of a 24-well tissue culture plate. All incubations were at 37°C under anaerobic conditions. After 1 min of shaking, OD_{600} readings were recorded every 10 min for 12 h using a BioTek Power Wave plate reader (all OD_{600} data and doubling time calculations are provided in Table S1).

Doubling times were calculated for each strain on a segment of the logarithmic growth phase using the exponential growth equation [$y = y_0 \cdot \exp(k \cdot x)$], with y being OD_{600}, y_0 being OD_{600} at time zero, and k being rate constant expressed in inversed minutes, with a least-squares fit, as implemented in Prism software (64-bit version 8.2.0 for Windows; GraphPad Software, Inc., San Diego, CA), and are presented as the average from at least two experiments (see the details in Table S1). The OD_{600} data were graphed using Prism software after the data were transformed by averaging the values for 5 neighbors and using zero-order smoothing.

Competitive colonization assays in gnotobiotic mice. Mouse studies were approved by the Institutional Animal Care and Use Committee (IACUC) of Brigham and Women's Hospital and complied with all relevant ethical regulations for animal testing and research. Gnotobiotic mice were obtained from and maintained in the Harvard Digestive Diseases Center gnotobiotic core facility at Brigham and Women's Hospital and housed in sterile OptiMICE cages (Animal Care Systems, Centennial, CO). All experiments were performed using Swiss Webster germfree mice that were 5 to 8 weeks old. For each experiment, both male and female mice (groups of three male and three female mice) were used. To differentiate the strains for quantification, the WT *B. fragilis* TM4000 strain was made tetracycline resistant by introduction of pNBU2-*bla-tetQ* into the *attB2* tRNA-Ser site, and the mutant strains were made erythromycin resistant by integration of pNBU2-*bla-ermGb*. For experiments with complemented mutant strains, the pNBU2-*bla-ermGb* constructs containing the cloned genes for complementation were similarly integrated into the *attB2* tRNA-Ser site. Strains were grown to an OD_{600} of approximately 0.6 and mixed at a 1:1 ratio, with the final percentage of each strain in the inoculum being determined by plating,

as reported in Fig. 5 and Table S2. Mice were gavaged with 200 μl of the bacterial mixtures, and 7 days later, fresh fecal samples were collected, diluted in sterile phosphate-buffered saline, and plated on BHIS medium plates. After colony growth, the bacteria were replica plated onto two plates containing either tetracycline or erythromycin to determine the exact percentage of each strain in the feces (Fig. 5; Table S2). A one-sample *t* test was performed using the arcsine-transformed values of the proportions of the WT and mutant strains present in the samples on days 1 and 7. The Δ*nqr* mutant competition data set had no standard error since there were no Δ*nqr* mutant colonies detected, so the value 1E−13 was added to one sample so that the values of the *t* test could be computed.

Data availability. Plasmid pLGB36 has been deposited in Addgene under accession no. 135621 for distribution to the scientific community.

SUPPLEMENTAL MATERIAL

Supplemental material is available online only.

FIG S1, TIF file, 0.9 MB.

TABLE S1, XLSX file, 0.1 MB.

TABLE S2, XLSX file, 0.01 MB.

TABLE S3, DOCX file, 0.02 MB.

TABLE S4, DOCX file, 0.01 MB.

ACKNOWLEDGMENTS

We thank V. Yeliseyev and R. Perez-Gonzales for assistance with gnotobiotic mouse work, the CBIS core facilities at RPI, and Joel Morgan for the critical reading of the manuscript and many suggestions.

The gnotobiotic mouse facility is supported by NIH grant P30DK034854 to the Massachusetts Host-Microbiome Center at Brigham and Women's Hospital, with additional funding coming from the Massachusetts Life Sciences Center. L. M. Matano received support from NIH grant T32 AI007061. This work was by supported by Public Health Service grant R01AI132580 from the National Institutes of Health, National Institute of Allergy and Infectious Diseases. L. E. Comstock received support from National Institute of Allergy and Infectious Diseases grant R01AI120633.

The funders had no role in study design, data collection and interpretation, or the decision to submit the work for publication.

We declare no conflict of interest.

REFERENCES

1. Blaser MJ, Cardon ZG, Cho MK, Dangl JL, Donohue TJ, Green JL, Knight R, Maxon ME, Northen TR, Pollard KS, Brodie EL. 2016. Toward a predictive understanding of Earth's microbiomes to address 21st century challenges. mBio 7:e00714-16. https://doi.org/10.1128/mBio.00714-16.
2. McGlynn SE, Chadwick GL, Kempes CP, Orphan VJ. 2015. Single cell activity reveals direct electron transfer in methanotrophic consortia. Nature 526:531–535. https://doi.org/10.1038/nature15512.
3. Stacy A, Fleming D, Lamont RJ, Rumbaugh KP, Whiteley M, Stacy A, Fleming D, Lamont RJ, Rumbaugh KP, Whiteley M. 2016. A commensal bacterium promotes virulence of an opportunistic pathogen via cross-respiration. mBio 7:e00782-16.
4. Hammer ND, Reniere ML, Cassat JE, Zhang Y, Hirsch AO, Hood MI, Skaar EP. 2013. Two heme-dependent terminal oxidases power *Staphylococcus aureus* organ-specific colonization of the vertebrate host. mBio 4:e00241-13. https://doi.org/10.1128/mBio.00241-13.
5. Lan L, Cheng A, Dunman PM, Missiakas D, He C. 2010. Golden pigment production and virulence gene expression are affected by metabolisms in *Staphylococcus aureus*. J Bacteriol 192:3068–3077. https://doi.org/10.1128/JB.00928-09.
6. Rivera-Chávez F, Zhang LF, Faber F, Lopez CA, Byndloss MX, Olsan EE, Xu G, Velazquez EM, Lebrilla CB, Winter SE, Bäumler AJ. 2016. Depletion of butyrate-producing *Clostridia* from the gut microbiota drives an aerobic luminal expansion of *Salmonella*. Cell Host Microbe 19:443–454. https://doi.org/10.1016/j.chom.2016.03.004.
7. Lopez CA, Kingsbury DD, Velazquez EM, Bäumler AJ. 2014. Collateral damage: microbiota-derived metabolites and immune function in the antibiotic era. Cell Host Microbe 16:156–163. https://doi.org/10.1016/j.chom.2014.07.009.
8. Louis P, Hold GL, Flint HJ. 2014. The gut microbiota, bacterial metabolites and colorectal cancer. Nat Rev Microbiol 12:661–672. https://doi.org/10.1038/nrmicro3344.
9. Varel VH, Bryant MP. 1974. Nutritional features of *Bacteroides fragilis* subsp. *fragilis*. Appl Microbiol 28:251–257.
10. Hooper LV, Stappenbeck TS, Hong CV, Gordon JI. 2003. Angiogenins: a new class of microbicidal proteins involved in innate immunity. Nat Immunol 4:269–273. https://doi.org/10.1038/ni888.
11. Hooper LV, Littman DR, Macpherson AJ. 2012. Interactions between the microbiota and the immune system. Science 336:1268–1273. https://doi.org/10.1126/science.1223490.
12. Kau AL, Ahern PP, Griffin NW, Goodman AL, Gordon JI. 2011. Human nutrition, the gut microbiome and the immune system. Nature 474:327–336. https://doi.org/10.1038/nature10213.
13. Mayer EA, Knight R, Mazmanian SK, Cryan JF, Tillisch K. 2014. Gut microbes and the brain: paradigm shift in neuroscience. J Neurosci 34:15490–15496. https://doi.org/10.1523/JNEUROSCI.3299-14.2014.
14. Nicholson JK, Holmes E, Kinross J, Burcelin R, Gibson G, Jia W, Pettersson S. 2012. Host-gut microbiota metabolic interactions. Science 336:1262–1267. https://doi.org/10.1126/science.1223813.
15. Stappenbeck TS, Hooper LV, Gordon JI. 2002. Developmental regulation of intestinal angiogenesis by indigenous microbes via Paneth cells. Proc Natl Acad Sci U S A 99:15451–15455. https://doi.org/10.1073/pnas.202604299.
16. Tang WH, Hazen SL. 2014. The contributory role of gut microbiota in cardiovascular disease. J Clin Invest 124:4204–4211. https://doi.org/10.1172/JCI72331.
17. Faith JJ, Guruge JL, Charbonneau M, Subramanian S, Seedorf H, Goodman AL, Clemente JC, Knight R, Heath AC, Leibel RL, Rosenbaum M, Gordon JI. 2013. The long-term stability of the human gut microbiota. Science 341:1237439. https://doi.org/10.1126/science.1237439.

18. Koropatkin NM, Cameron EA, Martens EC. 2012. How glycan metabolism shapes the human gut microbiota. Nat Rev Microbiol 10:323–335. https://doi.org/10.1038/nrmicro2746.
19. Poole RK, Cook GM. 2000. Redundancy of aerobic respiratory chains in bacteria? Routes, reasons and regulation. Adv Microb Physiol 43:165–224. https://doi.org/10.1016/s0065-2911(00)43005-5.
20. Kerscher S, Dröse S, Zickermann V, Brandt U. 2008. The three families of respiratory NADH dehydrogenases. Results Probl Cell Differ 45:185–222. https://doi.org/10.1007/400_2007_028.
21. Trumpower BL, Gennis RB. 1994. Energy transduction by cytochrome complexes in mitochondrial and bacterial respiration: the enzymology of coupling electron transfer reactions to transmembrane proton translocation. Annu Rev Biochem 63:675–716. https://doi.org/10.1146/annurev.bi.63.070194.003331.
22. Kröger A, Geisler V, Lemma E, Theis F, Lenger R. 1992. Bacterial fumarate respiration. Arch Microbiol 158:311–314. https://doi.org/10.1007/BF00245358.
23. Meehan BM, Malamy MH. 2012. Fumarate reductase is a major contributor to the generation of reactive oxygen species in the anaerobe *Bacteroides fragilis*. Microbiology 158:539–546. https://doi.org/10.1099/mic.0.054403-0.
24. Frigaard NU, Dahl C. 2009. Sulfur metabolism in phototrophic sulfur bacteria. Adv Microb Physiol 54:103–200. https://doi.org/10.1016/S0065-2911(08)00002-7.
25. Stewart V. 1988. Nitrate respiration in relation to facultative metabolism in enterobacteria. Microbiol Rev 52:190–232.
26. Barquera B, Hellwig P, Zhou W, Morgan JE, Häse CC, Gosink KK, Nilges M, Bruesehoff PJ, Roth A, Lancaster CRD, Gennis RB. 2002. Purification and characterization of the recombinant Na^+-translocating NADH:quinone oxidoreductase from *Vibrio cholerae*. Biochemistry 41:3781–3789. https://doi.org/10.1021/bi011873o.
27. Crofts AR, Hong S, Ugulava N, Barquera B, Gennis R, Guergova-Kuras M, Berry EA. 1999. Pathways for proton release during ubihydroquinone oxidation by the bc(1) complex. Proc Natl Acad Sci U S A 96:10021–10026. https://doi.org/10.1073/pnas.96.18.10021.
28. Friedrich T, Stolpe S, Schneider D, Barquera B, Hellwig P. 2005. Ion translocation by the *Escherichia coli* NADH:ubiquinone oxidoreductase (complex I). Biochem Soc Trans 33:836–839. https://doi.org/10.1042/BST0330836.
29. Wikström M. 2004. Cytochrome c oxidase: 25 years of the elusive proton pump. Biochim Biophys Acta 1655:241–247. https://doi.org/10.1016/j.bbabio.2003.07.013.
30. Sazanov LA. 2015. A giant molecular proton pump: Structure and mechanism of respiratory complex I. Nat Rev Mol Cell Biol 16:375–388. https://doi.org/10.1038/nrm3997.
31. Hunte C, Palsdottir H, Trumpower BL. 2003. Protonmotive pathways and mechanisms in the cytochrome bc_1 complex. FEBS Lett 545:39–46. https://doi.org/10.1016/s0014-5793(03)00391-0.
32. Konings WN. 2006. Microbial transport: adaptations to natural environments. Antonie Van Leeuwenhoek 90:325–342. https://doi.org/10.1007/s10482-006-9089-3.
33. Jung H. 2001. Towards the molecular mechanism of Na^+/solute symport in prokaryotes. Biochim Biophys Acta 1505:131–143. https://doi.org/10.1016/S0005-2728(00)00283-8.
34. Maloney PC, Kashket ER, Wilson TH. 1974. A protonmotive force drives ATP synthesis in bacteria. Proc Natl Acad Sci U S A 71:3896–3900. https://doi.org/10.1073/pnas.71.10.3896.
35. Dimroth P. 1994. Bacterial sodium ion-coupled energetics. Antonie Van Leeuwenhoek 65:381–395. https://doi.org/10.1007/bf00872221.
36. Schneider D, Pohl T, Walter J, Dorner K, Kohlstadt M, Berger A, Spehr V, Friedrich T. 2008. Assembly of the *Escherichia coli* NADH:ubiquinone oxidoreductase (complex I). Biochim Biophys Acta 1777:735–739. https://doi.org/10.1016/j.bbabio.2008.03.003.
37. Efremov RG, Sazanov LA. 2011. Structure of the membrane domain of respiratory complex I. Nature 476:414–420. https://doi.org/10.1038/nature10330.
38. Baradaran R, Berrisford JM, Minhas GS, Sazanov LA. 2013. Crystal structure of the entire respiratory complex I. Nature 494:443–448. https://doi.org/10.1038/nature11871.
39. Reyes-Prieto A, Barquera B, Juárez O. 2014. Origin and evolution of the sodium pumping NADH:quinone oxidoreductase. PLoS One 9:e96696. https://doi.org/10.1371/journal.pone.0096696.
40. Barquera B. 2014. The sodium pumping NADH:quinone oxidoreductase (Na^+-NQR), a unique redox-driven ion pump. J Bioenerg Biomembr 46:289–298. https://doi.org/10.1007/s10863-014-9565-9.
41. Belevich NP, Bertsova YV, Verkhovskaya ML, Baykov AA, Bogachev AV. 2016. Identification of the coupling step in Na^+-translocating NADH:quinone oxidoreductase from real-time kinetics of electron transfer. Biochim Biophys Acta 1857:141–149. https://doi.org/10.1016/j.bbabio.2015.12.001.
42. Juárez O, Morgan JE, Nilges MJ, Barquera B. 2010. Energy transducing redox steps of the Na^+-pumping NADH:quinone oxidoreductase from *Vibrio cholerae*. Proc Natl Acad Sci U S A 107:12505–12510. https://doi.org/10.1073/pnas.1002866107.
43. Heikal A, Nakatani Y, Dunn E, Weimar MR, Day CL, Baker EN, Lott JS, Sazanov LA, Cook GM. 2014. Structure of the bacterial type II NADH dehydrogenase: a monotopic membrane protein with an essential role in energy generation. Mol Microbiol 91:950–964. https://doi.org/10.1111/mmi.12507.
44. Caspari D, Macy JM. 1983. The role of carbon dioxide in glucose metabolism of *Bacteroides fragilis*. Arch Microbiol 135:16–24. https://doi.org/10.1007/bf00419476.
45. Macy JM, Probst I. 1979. The biology of gastrointestinal *Bacteroides*. Annu Rev Microbiol 33:561–594. https://doi.org/10.1146/annurev.mi.33.100179.003021.
46. Macy JM, Ljungdahl LG, Gottschalk G. 1978. Pathway of succinate and propionate formation in *Bacteroides fragilis*. J Bacteriol 134:84–91.
47. Macy JM, Probst I, Gottschalk G. 1975. Evidence for cytochrome involvement in fumarate reduction and adenosine 5′ triphosphate synthesis by *Bacteroides fragilis* grown in the presence of hemin. J Bacteriol 123:436–442.
48. Baughn AD, Malamy MH. 2003. The essential role of fumarate reductase in haem-dependent growth stimulation of *Bacteroides fragilis*. Microbiology 149:1551–1558. https://doi.org/10.1099/mic.0.26247-0.
49. Baughn AD, Malamy MH. 2004. The strict anaerobe *Bacteroides fragilis* grows in and benefits from nanomolar concentrations of oxygen. Nature 427:441–444. https://doi.org/10.1038/nature02285.
50. Van Hellemond JJ, Tielens A. 1994. Expression and functional properties of fumarate reductase. Biochem J 304:321–331. https://doi.org/10.1042/bj3040321.
51. Moparthi VK, Hägerhäll C. 2011. The evolution of respiratory chain complex I from a smaller last common ancestor consisting of 11 protein subunits. J Mol Evol 72:484–497. https://doi.org/10.1007/s00239-011-9447-2.
52. Franke T, Deppenmeier U. 2018. Physiology and central carbon metabolism of the gut bacterium *Prevotella copri*. Mol Microbiol 109:528–540. https://doi.org/10.1111/mmi.14058.
53. Deusch S, Scheicher L, Seifert J, Steuber J. 2019. Occurrence and function of the Na^+ translocating NADH:quinone oxidoreductase in *Prevotella* spp. Microorganisms 7:e117. https://doi.org/10.3390/microorganisms7050117.
54. Duran-Pinedo AE, Nishikawa K, Duncan MJ. 2007. The RprY response regulator of *Porphyromonas gingivalis*. Mol Microbiol 64:1061–1074. https://doi.org/10.1111/j.1365-2958.2007.05717.x.
55. Li Y, Krishnan K, Duncan MJ. 2018. Post-translational regulation of a *Porphyromonas gingivalis* regulator. J Oral Microbiol 10:1487743. https://doi.org/10.1080/20002297.2018.1487743.
56. Albenberg L, Esipova TV, Judge CP, Bittinger K, Chen J, Laughlin A, Grunberg S, Baldassano RN, Lewis JD, Li H, Thom SR, Bushman FD, Vinogradov SA, Wu GD. 2014. Correlation between intraluminal oxygen gradient and radial partitioning of intestinal microbiota in humans and mice. Gastroenterology 147:1055–1063. https://doi.org/10.1053/j.gastro.2014.07.020.
57. Puustinen A, Finel M, Haltia T, Gennis RB, Wikström M. 1991. Properties of the two terminal oxidases of *Escherichia coli*. Biochemistry 30:3936–3942. https://doi.org/10.1021/bi00230a019.
58. Borisov VB, Gennis RB, Hemp J, Verkhovsky MI. 2011. The cytochrome bd respiratory oxygen reductases. Biochim Biophys Acta 1807:1398–1413. https://doi.org/10.1016/j.bbabio.2011.06.016.
59. Matsushita K, Ohnishi T, Kaback HR. 1987. NADH-ubiquinone oxidoreductases of the *Escherichia coli* aerobic respiratory chain. Biochemistry 26:7732–7737. https://doi.org/10.1021/bi00398a029.
60. Zambrano MM, Kolter R. 1993. *Escherichia coli* mutants lacking NADH dehydrogenase I have a competitive disadvantage in stationary phase. J Bacteriol 175:5642–5647. https://doi.org/10.1128/jb.175.17.5642-5647.1993.
61. Zhou WD, Bertsova YV, Feng BT, Tsatsos P, Verkhovskaya ML, Gennis RB, Bogachev AV, Barquera B. 1999. Sequencing and preliminary characterization of the Na^+-translocating NADH:ubiquinone oxidoreductase from *Vibrio harveyi*. Biochemistry 38:16246–16252. https://doi.org/10.1021/bi991664s.

62. Chatzidaki-Livanis M, Geva-Zatorsky N, Comstock LE. 2016. *Bacteroides fragilis* type VI secretion systems use novel effector and immunity proteins to antagonize human gut *Bacteroidales* species. Proc Natl Acad Sci U S A 113:3627–3632. https://doi.org/10.1073/pnas.1522510113.
63. Häse CC, Barquera B. 2001. Role of sodium bioenergetics in *Vibrio cholerae*. Biochim Biophys Acta 1505:169–178. https://doi.org/10.1016/S0005-2728(00)00286-3.
64. Häse CC, Fedorova ND, Galperin MY, Dibrov PA. 2001. Sodium ion cycle in bacterial pathogens: evidence from cross-genome comparisons. Microbiol Mol Biol Rev 65:353–370. https://doi.org/10.1128/MMBR.65.3.353-370.2001.
65. Weerakoon DR, Olson JW. 2008. The *Campylobacter jejuni* NADH: ubiquinone oxidoreductase (complex I) utilizes flavodoxin rather than NADH. J Bacteriol 190:915–925. https://doi.org/10.1128/JB.01647-07.
66. Baughn AD, Malamy MH. 2002. A mitochondrial-like aconitase in the bacterium *Bacteroides fragilis*: implications for the evolution of the mitochondrial Krebs cycle. Proc Natl Acad Sci U S A 99:4662–4667. https://doi.org/10.1073/pnas.052710199.
67. Coyne MJ, Roelofs KG, Comstock LE. 2016. Type VI secretion systems of human gut Bacteroidales segregate into three genetic architectures, two of which are contained on mobile genetic elements. BMC Genomics 17:58. https://doi.org/10.1186/s12864-016-2377-z.
68. Garcia-Bayona L, Comstock LE. 2019. Streamlined genetic manipulation of diverse *Bacteroides* and *Parabacteroides* isolates from the human gut microbiota. mBio 10:e01762-19. https://doi.org/10.1128/mBio.01762-19.
69. Coyne MJ, Béchon N, Matano LM, McEneany VL, Chatzidaki-Livanis M, Comstock LE. 2019. A family of anti-Bacteroidales peptide toxins widespread in the human gut microbiota. Nat Commun 10:3460. https://doi.org/10.1038/s41467-019-11494-1.
70. Ramotar K, Conly JM, Chubb H, Louie TJ. 1984. Production of menaquinones by intestinal anaerobes. J Infect Dis 150:213–218. https://doi.org/10.1093/infdis/150.2.213.
71. Sheppard CA, Trimmer EE, Matthews RG. 1999. Purification and properties of NADH-dependent 5,10-methylenetetrahydrofolate reductase (MetF) from *Escherichia coli*. J Bacteriol 181:718–725.